Novel Inhibitors of the Gardos Channel for the Treatment of Sickle Cell Disease

Grant A. McNaughton-Smith,[†] J. Ford Burns,[†] Jonathan W. Stocker,*[,†] Gregory C. Rigdon,[†] Christopher Creech,[†] Susan Arrington,[†] Tara Shelton,[†] and Lucia de Franceschi[‡]

Icagen, Inc., Post Office Box 14487, Research Triangle Park, North Carolina 27709, and Department of Internal Medicine, University of Verona, Italy

Received June 8, 2007

Sickle cell disease (SCD) is a hereditary condition characterized by deformation of red blood cells (RBCs). This phenomenon is due to the presence of abnormal hemoglobin that polymerizes upon deoxygenation. This effect is exacerbated when dehydrated RBCs experience a loss of both water and potassium salts. One critical pathway for the regulation of potassium efflux from RBCs is the Gardos channel, a calcium-activated potassium channel. This paper describes the synthesis and biological evaluation of a series of potent inhibitors of the Gardos channel. The goal was to identify compounds that were potent and selective inhibitors of the channel but had improved pharmacokinetic properties compared to **1**, Clotrimazole. Several triarylamides such as **10** and **21** were potent inhibitors of the Gardos channel (IC_{50} of <10 nM) and active in a mouse model of SCD. Compound **21** (ICA-17043) was advanced into phase 3 clinical trials for SCD.

Introduction

Sickle cell disease (SCD[a]) is a debilitating, hereditary disease caused by expression of a point mutation in the β-globin gene of hemoglobin. This mutation leads to the production of abnormal hemoglobin (HbS), which polymerizes when it is deoxygenated, eventually leading to the formation of sickle-shaped red blood cells (RBCs), which are involved in an interruption of blood flow (vaso-occlusion) to various organs and tissues. Individuals with SCD have episodes of painful vaso-occlusive crises, acute chest syndrome, priapism, pulmonary hypertension, stroke, and many other acute and chronic disorders that ultimately lead to a decreased life expectancy.[1,2]

The rate of RBC sickling is dramatically affected by the intracellular concentration of HbS.[3,4] Studies have shown that by preventing the dehydration of RBCs, and thus preventing increases in the HbS concentration, RBC sickling can be reduced.[5] Because RBC dehydration is initiated by the loss of intracellular KCl and $KHCO_3$ followed by the osmotically driven loss of water, inhibiting the transport of K^+ from the RBCs should reduce cell dehydration and, therefore, decrease the formation of sickled cells.

The Gardos channel, a calcium activated K^+ channel of intermediate conductance,[6–8] has been shown to be one of the main routes for K^+ loss in RBCs. Clotrimazole **1**, a small molecule inhibitor of the Gardos channel (Figure 1), was shown to block RBC dehydration[9–12] and was efficacious in a mouse model of SCD (SAD-1 mouse model).[13,14] The use of this compound for the long-term SCD therapy is limited by several factors including its inhibition of mammalian cytochrome P-450s (particularly CYP3A4),[15] its relatively short in vivo plasma half-life,[16] the toxicity experienced upon repetitive dosing,[17] and inhibition of several cardiac ion channels including hERG.[18]

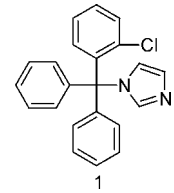

1

Figure 1. Clotrimazole, **1**.

Chemistry

The chemistry plan had several key goals: the first was to identify those structural features required for blocking the Gardos channel; the second was to optimize the selectivity for the target channel; and the third was to improve the pharmacokinetic properties. The initial sets of compounds were derivatives of **1**, in which the imidazole moiety was replaced with other functional groups such as amides and reverse amides (see Supporting Information). The compounds were prepared using standard solution phase parallel synthesis techniques. In the first set, four commercially available aromatic acids (triphenylacetic acid, phenyl acetic acid, diphenylacetic acid, and 9-phenylflurenyl) and one isocyanate (triphenylisocyante) were coupled with the 12 amines and 1 alcohol, resulting in a set of 65 compounds. In addition, a set of the corresponding inverse amides/sulfonamides were generated in a similar fashion by reacting triphenylmethylamine or flurenylamine with a set of acid chlorides and one sulfonyl chloride.

Several additional compounds were made to further define the structure–activity relationships. For example, compounds **4** and **7** (Scheme 1) were designed to investigate the role of the amide and its spatial relationship to the three aryl rings. The addition of ethanolamine to the activated acid of **2** gave the amide **3**, which was converted to the oxazolidine in high yield using Burgess reagent.[19] The constrained amide **7** was obtained by condensing the isatin **6** with benzene using an excess of triflic acid.[20]

The substituted triphenylmethane amides (Table 2) were obtained as outlined in Scheme 2. Addition of phenylmagnesium bromide to the commercially available benzophenones **8** afforded the substituted triphenylmethane alcohols, which were transformed into the triphenylmethane chlorides using a 3–5-fold excess of acetyl chloride. These key intermediates were not purified, but directly converted to the cyano derivatives **9** using a slight excess of copper. Hydrolysis methods employing a basic medium did not generate significant quantities of the

* To whom correspondence should be addressed. Tel.: 919-941-5206. Fax: 919-941-0813. E-mail: jstocker@icagen.com.

[†] Icagen, Inc.

[‡] University of Verona.

[a] Abbreviations: SCD, sickle cell disease; RBC, red blood cell; HbS, abnormal hemoglobin.

10.1021/jm070663s CCC: $40.75
Published on Web 01/31/2008

Scheme 1. Preparation of Amide Bioisosteres and Cyclic Amides Reagents[a]

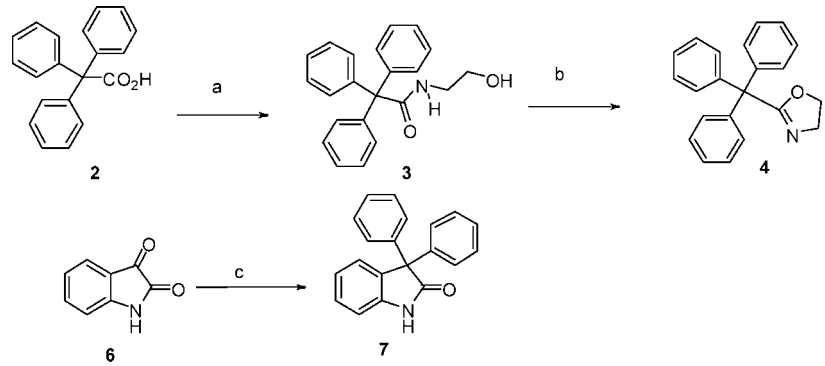

[a] Reagents and conditions: (a) HOBt, Et_3N, $(EtO)_2POCl$, 1 h, then $H_2NCH_2CH_2OH$; (b) Burgess reagent, THF, 50 °C; (c) 2 mol equiv C_6H_6, triflic acid, 14 h.

Table 1. Inhibition of Ionomycin Stimulated ^{86}Rb efflux (IC_{50} Values, Gardos Channel) for Selected Triphenylmethane Derivatives

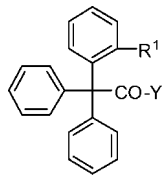

ID#	R^1	Y	RBC's IC_{50}[a] (μM)
1	clotrimazole		0.36 ± 0.07
2	H	OH	>10
15	H	OMe	0.33 ± 0.1
5	H	NH_2	0.07 ± 0.004
16	H	NHMe	0.55 ± 0.3
17	H	NHEt	1.75 ± 0.8
18	H	NMe_2	3.15 ± 2.3
19	Cl	NH_2	0.02 ± 0.01

[a] Number of measurements = 4.

Table 2. Summary of ADME Data for Compounds **10** and **21**

cmpd	RS9[a]	Sol (μm)	*F*% (rat)	$T_{1/2}$ (h)	T_{max} (h)	C_{max} (ng/ml)
10	40%	5.8	35	2.5	2	250
21	51%	3.8	51	1.0	4	400

[a] Percent remaining after incubation with S9.

desired amide. However, strongly acidic conditions at elevated temperatures efficiently converted the nitriles into the amides (**10**, **21**–**33**).[21]

The 2,2′ and 3,3′ difluorinated benzophenones (**14a** and **14b**) were not commercially available and were prepared as shown in Scheme 2. Addition of ethylformate to the appropriate aryllithium, generated in situ via lithium−halogen exchange,[22] afforded the intermediate alcohol **13a**. Oxidation of **13a** using PCC gave the desired benzophenone **14a** in good overall yield. The 3-difluoro benzophenone analog **14b** was prepared using the same procedure.

Results and Discussion

The current study focused on identifying the structural features of **1** responsible for the Gardos channel inhibitory activity, while minimizing or eliminating CYP450 enzyme inhibition and metabolic stability issues. The imidazole moiety in **1** was believed to contribute to both the inhibition of the CYP450 metabolizing enzymes and the compound's relatively short half-life. The short half-life was believed to result from the known susceptibility of the C−N bond (the bond between the triphenylmethane and imidazole group) to undergo hydrolysis.[16]

The monoaryl and diaryl amide derivatives that were prepared using solution phase techniques were all inactive when tested against the Gardos Channel (<50% inhibition at 10 μM as measured by $^{86}Rb^+$ efflux—data not shown). However, those compounds (**2**, **5**, **15**–**19**) resulting from the coupling of the triphenylacetic acid with small amines and alcohols were active (Figure 2, Table 1). The difference in activity between the acid **2** and the methyl ester **15** was striking and indicated that changes in pK_a and the ability of the carbonyl group to participate in hydrogen bonding was a possible factor. The most significant jump in potency was seen with compound **5**, in which the carboxylic acid was converted to the primary amide. This compound was 7-fold more potent than **1**. Introduction of substituents on the amide nitrogen of **5** (compounds **16**, **17**, and **18**) led to reduced activity. For example, **16** was 8-fold less active than **5**, the ethyl derivative **17** was even less active, while the dimethylated amide **18** possessed only low micromolar activity.

The Gardos channel inhibition data for the triphenylmethane derivatives indicated that small functional groups having the ability to act as hydrogen bond acceptors were preferred. Based upon this theory, the constrained cyclic amide **7** and the amide bioisostere **4** were synthesized to investigate the spatial role of the amide with the triphenyl system and the impact of the amide tautomeric form. The oxazolidine **4** (Scheme 1) possessed only weak inhibitory activity (IC_{50} = 4.3 ± 0.4 μM) perhaps due in part to the increased steric bulk of the ring system, while the constrained amide **7** was surprisingly devoid of inhibitory activity (<20% inhibition at 10 μM).

To investigate the importance of the chlorine substituent present in **1**, the corresponding 2-chloro derivative of **5** was prepared. Compound **19** was found to be 4-fold more potent than **5** (IC_{50} of 15 nM vs 69 nM).

Prior to embarking upon the synthesis of additional analogs, several of the more potent compounds (**5**, **16**, and **19**) were tested against the hERG channel. In summary, none of the compounds significantly inhibited this important cardiac ion channel (<20% inhibition at 10 μM). Additional testing against CYP3A4 showed that none of the compounds inhibited CYP3A4 (<20% inhibition at 10 μM).

Having substantially improved both in vitro potency against the cloned channel and ion channel selectivity compared to **1**, we turned our attention to improving the in vivo stability and, thus, bioavailability of the series. Compound **19** was administered both intravenously and orally to rats (Figure 2). When given IV, **19** had a relatively short half-life ($t_{1/2}$ = 15 min), while oral administration lead to very low plasma

Scheme 2. General Procedure for the Preparation of Triphenylmethane Amides[a]

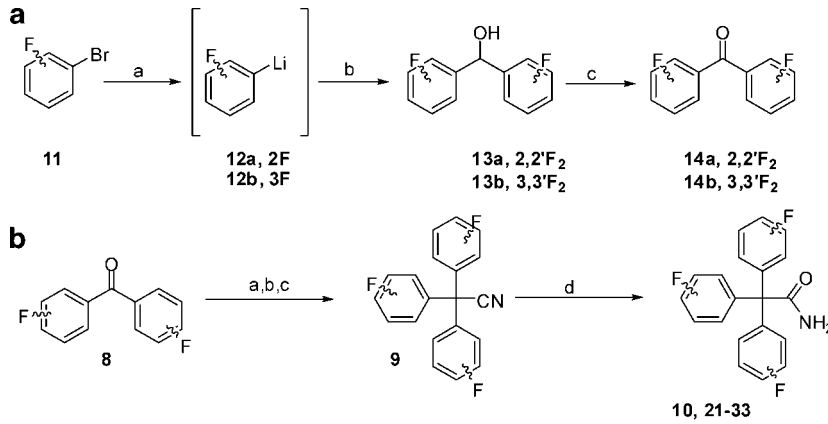

[a] Reagents and conditions for (**a**): (a) *n*-BuLi, THF, −78 °C, 1 h; (b) HCO_2Et, 1 h, −78 to 0 °C; (c) PCC, DCM, 12 h, rt. Reagents and conditions for (**b**): (a) fluoro-substituted phenylMgBr, THF, or *t*-BuOMe, rt, 4 h; (b) AcCl, DCM, rt, 12 h; (c) CuCN, 140 °C, 3 h; (d) 1:1, H_2SO_4/HOAc, 120 °C, 3 h.

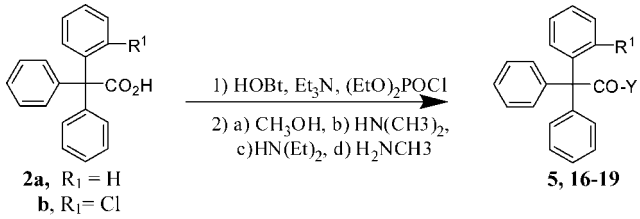

Figure 2. Synthesis of aromatic amides related to **1**.

concentrations. The bioavailability of **19** was calculated to be <5%, presumably due to a rapid rate of elimination. Although amide hydrolysis was a potential liability, the nature and size of the neighboring triphenylmethane group was considered to be a hindrance to this metabolic route. However, the three unprotected phenyl rings were considered potential sites for oxidative metabolism.

Initially, we examined the effect on metabolism of fluorine substitution at the *ortho* and *para* positions of the phenyl rings. Fluorine was chosen as one of the first substituents due to its small size and strong electron-withdrawing capability. The 2,4′-disubstituted and 4,4′-disubstituted compounds **10** and **21**, respectively, were prepared. Both compounds retained their potency against the RBC Gardos channel as well as their selectivity against a collection of ion channels. In addition, these compounds did not have CYP3A4 activity at high concentrations (<20% inhibition at 10 μM).

Compound **10** was found to be orally bioavailable ($F = 35\%$) in a rat pharmacokinetic study with a $T_{1/2}$ of 150 min. In addition, compound **21** in which two of the *para* positions were substituted with fluorine was more stable ($T_{1/2} = 66$ min) than **19** and considerably more bioavailable in rats ($F = 51\%$). The data is summarized in Table 2. In addition, the improved pharmacokinetics were confirmed in mice.

Based upon the encouraging data obtained with **10** and **21**, a series of fluorinated analogues were synthesized (Table 3). All of the fluorine containing amides had good inhibitory activity versus the native Gardos channel in RBCs. However, there were notable differences in aqueous solubility and susceptibility to metabolism when incubated with rat S9 fractions (Table 3). Although no clear trends were observed among mono-, di-, and trisubstituted compounds, those containing a fluorine in the *meta* position were generally found to be more prone to oxidative metabolism.

Compounds **10** and **21** remained as the prime candidates for in vivo testing in the SAD-1 mouse model of sickle cell disease.[13,14] In this model, an inhibitor of the Gardos channel should result in less RBC dehydration and would be expected to decrease the mean corpuscular hemoglobin concentration (MCHC) and increase the hematocrit (Hct) levels. Dosing of SAD-1 mice with **10** (20 mg/kg) twice a day for 14 days via oral gavage produced a reduction in the MCHC on day 7 (first analysis day) as well as a significant increase in hematocrit. In addition, the number of dense RBCs was reduced (Table 4).[23] Most important was the fact that all of the changes in hematological parameters were maintained throughout the course of the experiment. Compound **21** was also tested in the model. Due to its improved bioavailability and longer half-life, the animals were dosed with 10 mg/kg twice a day for 21 days. Hematological parameters were collected on days 11 and 21, with results similar to those obtained with compound **10** (Table 4). Compound **21**, ICA-17043, completed preclinical testing and

Table 3. In Vitro Activity of Fluorinated Triphenylmethane Amides

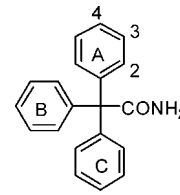

ID#	ring A	ring B	ring C	IC50 RBCs (nM)[a]	RS9[b,c] (%)	Sol[d,e] (μM)
10	2F	4F		9	40	5.8
21	4F	4F		12	56	3.8
22	4F	4F	2F	10	62	8.3
23	3F, 4F			14	63	4.3
24	2F, 4F			34	44	1.8
25	4F	4F	4F	14	25	2.6
26	2F	2F		30	48	>31
27	2F	2F	4F	15	46	6.8
28	3F	4F	4F	17	19	4.1
29	3F	3F	3F	13	36	3.4
30	2F			15	61	10.6
31	4F			40	58	2.9
32	3F	3F		30	43	1.2
33	3F	3F	4F	15	nd	nd
1				0.36	nd	nd

[a] Number of measurements = 2. The error in the RBC measurement is typically ±5 nM. [b] Percent remaining after incubation with rat S9 fraction for 2 h. [c] Number of measurements = 1 or 2. The error in the S9 fraction measurement is typically ±15%. [d] Solubility was measured using the Lipinski type method (ref 23). [e] Number of measurements = 2. The error in the solubility measurement is typically ±0.1 μM.

Table 4. Hematological Data Obtained from Administration of **10** (20 mg/kg, bid) and **21** (10 mg/kg, bid) in the SAD-1 Mouse Model[a]

measure		cmpd **10**	cmpd **21**
Gardos channel activity (mmol Rb/L of cells)	day 0	11 ± 1	12 ± 1
	day 7	4 ± 1	-
	day 11	-	3 ± 1
	day 14	2 ± 0.2	-
	day 21	-	1.5 ± 0.5
MCHC (g/dL)	day 0	40 ± 2	34 ± 1
	day 7	34 ± 1	-
	day 11	-	29.5 ± 1
	day 14	27 ± 0.4	-
	day 21	-	30.3 ± 1.5
Hct (%)	day 0	44.5 ± 0.3	43.5 ± 0.7
	day 7	44.5 ± 0.3	-
	day 11	-	50.9 ± 2.2
	day 14	47 ± 0.6	-
	day 21	-	49.9 ± 4.1

[a] The symbol "-" indicates no data were collected on these days.

has advanced into clinical trials as a potential treatment for individuals with SCD.[24]

Conclusions

A novel series of Gardos channel inhibitors with potent activity, selectivity, and excellent pharmacokinetic properties has been identified. Two of these compounds, **10** and **21**, were shown to improve hemodynamic parameters in an animal model of sickle cell disease.

Experimental Section

Melting points were determined with an Electrothermal IA9000 melting point apparatus and are uncorrected. Unless otherwise noted, starting materials were purchased from Aldrich Chemical Co. (Milwaukee, WI). The 2,2′- and 3,3′-difluorbenzophenones were prepared as described below. All other fluorinated benzophenones were commercially available. Reactions were run at room temperature under an atmosphere of argon, unless otherwise indicated. Organic phases from aqueous extractions were dried over Na_2SO_4, filtered, and concentrated. Reactions were monitored by TLC analysis on silica gel 60 F_{254}, with detection using UV light at 254 nM. Flash chromatography was performed on silica gel (particle size 32–63), and the column output was monitored with TLC. Elemental analyses, performed by Atlantic Microlabs, Atlanta, GA, were within ±0.4% of theoretical values. Nuclear magnetic resonance (NMR) spectra were recorded in either $CDCl_3$ or DMSO-d_6 solutions with a Varian (Gemini 2000) spectrometer using TMS as an internal standard. Mass spectral data were obtained on a PE SCIEX API150EX mass spectrometer. The yields quoted in this paper are isolated yields. The amount of DMSO in the solutions tested in vitro was not greater than 1% of the total volume. Cerep, Inc., Redmond, WA, performed the inhibitions of CYP3A4 enzymes.

All samples for the solubility, microsome, and in vivo studies were analyzed using online turbulent-flow "extraction" (Cohesive 2300 HTLC system including a CTC autosampler, an Agilent 1100 Binary LC pump, and an Agilent 1100 Quaternary LC pump). Mass spectra were obtained on a Micromass Quattro Ultima spectrometer.

All plasma samples with quantifiable concentrations were used in the pharmacokinetic calculations. Samples measuring below the lower limit of quantitation (LLOQ = 1 ng/mL) were considered as zeros. Noncompartmental analysis of plasma concentration data was accomplished using WinNonlin Professional Software (version 4.0.1, Pharsight Corporation, Mountain View, CA). The maximum plasma concentration (C_{max}) and time of maximum plasma concentration (T_{max}) were determined by observation of the data. The $AUC_{0-\infty}$ was calculated using the linear-log trapezoidal rule. Mean, standard deviation, minimum, median, and maximum values were calculated using Excel2000 (Microsoft Corporation). Plots of plasma concentration vs time were prepared using SigmaPlot 2001 for Windows (version 7, SPSS, Inc., Chicago, IL).

***N*-Methyl-2,2,2-triphenylacetamide (16).** A mixture of HOBt (281 mg, 2.1 mmol), Et_3N (0.87 mL, 6.3 mmol), and $(EtO)_2POCl$ (0.3 mL, 2.1 mmol) in dry THF (5 mL) was stirred at room temperature for 20 min. To the reaction was added **2a** (600 mg, 2.1 mmol), and the stirring continued for 1 h. Then a solution of methylamine in methanol (2.0 M, 1.25 mL, 2.5 mmol) was added, and the mixture was stirred for 1 h. To the resulting solution was added EtOAc (10 mL) and brine (10 mL), and the organic layers were separated, dried (Na_2SO_4), and concentrated. Purification by column chromatography (SiO_2, hexanes/EtOAc, 4:1) gave the desired product **16** as a white solid (0.587 g, 94%): ^{1}H NMR δ ($CDCl_3$) 7.36–7.21 (15H, m), 5.82 (1H, brs), and 2.84 (3H, d, J= 6 Hz); Anal. ($C_{22}H_{21}NO$) C, H, N.

The following compounds were prepared as described for **16**.

***N*-Ethyl-2,2,2-triphenylacetamide (17).** Compound **17** was obtained from ethylamine, as a white solid: ^{1}H NMR δ (DMSO-d_6) 7.31–7.17 (15H, m), 3.54 (2H, q, J= 7 Hz), and 1.32 (3H, t, J= 7 Hz); Anal. ($C_{22}H_{21}NO$) C, H, N.

***N*,*N*-Dimethyl-2,2,2-triphenylacetamide (18).** Compound **18** was obtained from dimethylamine, as a white solid: ^{1}H NMR δ (DMSO-d_6) 7.31–7.17 (15H, m), 3.05 (3H, s), and 2.35 (3H, s).

2,2,2-Triphenylacetamide (5). Compound **5** was obtained from ammonia in methanol, as a white solid: ^{1}H NMR δ (DMSO-d_6) 7.49 (1H, brs), 7.30–7.19 (15H, m), and 6.58 (1H, brs).

Triphenylacetic Acid Methyl Ester (15). Compound **15** was obtained from methanol, as a white solid: ^{1}H NMR δ (DMSO-d_6) 7.32–7.26 (10H, m), 7.17–7.14 (5H, m), and 3.80 (3H, s); Anal. ($C_{21}H_{18}O_2$) C, H, N.

***N*-(2-Hydroxy-ethyl)-2,2,2-triphenyl-acetamide (3).** A mixture of HOBt (135 mg, 1 mmol), Et_3N (0.42 mL, 3 mmol), and $(EtO)_2POCl$ (0.145 mL, 1 mmol) in dry THF (5 mL) was stirred at room temperature for 20 min, after which triphenylacetic acid (289 mg, 1 mmol) was added and the stirring continued for an additional 1 h. To the mixture was added ethanolamine (0.07 mL, 1.1 mmol), and after 1 h, EtOAc (10 mL) and brine (10 mL) were added. The organic layer was separated, dried (Na_2SO_4), and concentrated. Purification by column chromatography (SiO_2, hexanes/EtOAc; 1:1) gave **3** as a white solid (299 mg, 85%): ^{1}H NMR δ ($CDCl_3$) 7.34–7.21 (15H, m), 6.25 (1H, brs), 3.69 (2H, t, J = 5.0 Hz), 3.49 (2H, q, J = 5.5 Hz), and 2.05 (1H, brs).

2-Trityl-4,5-dihydrooxazole (4). To a solution of **3** (299 mg, 0.85 mmol) in THF (5 mL) was added (methoxycarbonylsulfamoyl)triethylammonium hydroxide (Burgess reagent; 300 mg, 1 mmol). The resulting solution was heated at 50 °C for 1.5 h, cooled to room temperature, and EtOAc (20 mL) was added. The organic layer was washed with aqueous 1 N HCl (20 mL), saturated aqueous solution of $NaHCO_3$ (20 mL), and brine (20 mL) and dried (Na_2SO_4). The solution was concentrated in vacuo and the crude product was purified bypassage thorough a short silica plug (hexanes/EtOAc, 2:1) to afford the desired product as a white solid (248 mg, 93%): ^{1}H NMR δ ($CDCl_3$) 7.31–7.26 (10H, m), 7.24–7.16 (5H, m), 4.34 (2H, t, J = 9.5 Hz), and 3.98 (2H, t, J = 9.5 Hz); Anal. ($C_{22}H_{19}NO$) C, H, N.

(2-Fluorophenyl)-(4-fluorophenyl)phenylacetamide (10). To a stirred solution of 2,4′-difluorobenzophenone (1.09 g, 5.0 mmol) in *t*-butylmethyl ether (12 mL) at room temperature was added dropwise phenylmagnesium bromide (1.83 mL, 5.5 mmol). After the addition was complete, the reaction was heated at reflux for 3 h, cooled to room temperature, and then poured onto cold 1.0 M HCl (aq; 0 °C, 20 mL). The organic layer was extracted with EtOAc (3 × 10 mL) and dried (Na_2SO_4). Concentration under reduced pressure gave the desired product (2-fluorophenyl)-(4-fluorophenyl)-phenylmethanol as a pale brown oil, which was used in the next reaction without any further purification.

To a 20% solution of acetyl chloride in dichloromethane (10 mL) at room temperature was added the crude (2-fluorophenyl)-(4-fluorophenyl)phenylmethanol (1.47 g, 5.0 mmol) from above. The resulting solution was stirred for 12 h, after which the solvent was removed by evaporation and toluene (2 × 20 mL) was

sequentially added to the residue and evaporated to afford crude 2-fluorophenyl-(4-fluorophenyl) phenylchloromethane.

To this crude material was added copper cyanide (0.50 g, 5.5 mmol), and the mixture was heated at 140 °C for 2.5 h. The reaction was cooled to approximately 110 °C, toluene (30 mL) was added, the slurry was stirred vigorously for 10 min and filtered, and the solvent was removed under reduced pressure. To the resulting crude material, hot hexane (30 mL) was added and the mixture was stirred vigorously for 30 min. Filtration and trituration with more hexane (2 × 30 mL) gave the desired cyano intermediate **9** as a white solid.

To the solid (**9**, 1.48 g, 5.0 mmol) at room temperature was added a solution of concentrated sulfuric acid (10 mL) and glacial acetic acid (10 mL). The resulting orange solution was stirred and heated at 130 °C for 3 h, cooled to 0 °C, and was neutralized by the dropwise addition of ammonium hydroxide. Water (30 mL) was added, and the aqueous layer was extracted with chloroform (3 × 30 mL). The organic fractions were combined and washed sequentially with water (2 × 10 mL) and brine (20 mL). The organic phase was dried (Na_2SO_4) and concentrated under reduced pressure to provide a light brown oil to which hexanes (30 mL) were added to the initiate precipitation. The precipitate was filtered and triturated with hot hexane (2 × 30 mL). Crystallization from hexane/dichloromethane gave the desired product **10** as a white crystalline solid (0.45 g, 1.4 mmol, 28%, 4 steps): ^{1}H NMR δ ($CDCl_3$) 7.39–7.26 (8H, m), 7.15–6.90 (5H, m), 5.83 (1H, brs), 5.72 (1H, brs); ^{19}F NMR δ ($CDCl_3$) −103.4 (1F, s), −115.8 (1F, s); mp 180–181 °C; Anal. ($C_{20}H_{15}F_2NO$) C, H, N.

Bis(4-fluorophenyl)phenylacetamide (21). To a stirring solution of 4,4′-difluorobenzophenone (20 g, 0.092 mol) in *t*-butylmethyl ether (150 mL) at room temperature was added phenylmagnesium bromide (100 mL, 0.1 mol) dropwise. After the addition was complete, the reaction was heated at reflux for 3 h, cooled to room temperature, and poured into ice cold aqueous 1.0 M HCl (100 mL). The organic layer was extracted with EtOAc (2 × 50 mL), dried (Na_2SO_4), and concentrated under reduced pressure to provide bis(4-fluorophenyl)phenylmethanol as a pale brown oil. The material was dried in vacuo for 2 h and was used in the next reaction without any further purification.

Bis(4-fluorophenyl)phenylmethanol (0.092 mol) was added to a 20% solution of acetyl chloride in dichloromethane (50 mL) at room temperature. The resulting purple solution was stirred for 12 h after which time the solvent was removed by evaporation. Toluene (100 mL) was added to the residue and then evaporated to afford crude bis(4-fluorophenyl)phenylchloromethane, which was used without further purification.

Copper cyanide (8.24 g, 0.11 mol) was added to the crude residue, and the mixture was heated at 140 °C for 3 h. The reaction was cooled to 100 °C and toluene (100 mL) was added. The resulting slurry was stirred vigorously for 10 min, cooled to room temperature, and filtered through a short plug of silica, and the solvent was removed under reduced pressure to afford a brown solid. Hot hexane (100 mL) was added to the powdered crude material and the mixture was stirred vigorously for 4 h. Filtration and trituration with additional hexane gave the desired bis(4-fluorophenyl)phenylacetonitrile as a white solid (18.9 g, 67%).

A solution of concentrated sulfuric acid (50 mL) and glacial acetic acid (50 mL) was added to bis(4-fluorophenyl)phenylacetonitrile (18.9 g, 0.06 mol) at room temperature. The resulting orange solution was stirred and heated at 130 °C for 3 h. The reaction was cooled to 0 °C, poured into ice–water (150 mL), and neutralized with ammonium hydroxide. The organics were extracted with chloroform (3 × 100 mL), combined, and washed with brine (2 × 50 mL). The organics were dried (Na_2SO_4) and concentrated under reduced pressure to afford a yellow-orange solid. The solid was stirred with hot hexane (100 mL) for 30 min and filtered. Crystallization from dichloromethane/hexane gave **21** as a white crystalline solid (16.9 g, 0.052 mol, 87%; 58% over 4 steps): ^{1}H NMR δ ($CDCl_3$) 7.37–7.20 (9H, m), 7.04–6.91 (4H, m), 5.81 (1H, brs), 5.71 (1H, brs); ^{19}F NMR δ ($CDCl_3$) −115.7 (F, m); mp 180–181 °C; Anal. ($C_{20}H_{15}F_2NO$) C, H, N.

The following compounds were prepared using the procedure described for compound **21**.

2-(2-Chlorophenyl)-2,2-diphenylethanamide (19). A mixture of **1** (0.5 g, 1.4 mmol) in 1.0 M HCl (2 mL) was refluxed for 2 h and then cooled. The residue was extracted with EtOAc (2 × 10 mL), and the organic layer was washed with brine (2 × 10 mL), dried (Na_2SO_4), and concentrated. The solid was recrystallized from hexanes to provide (2-chlorophenyl)diphenylmethanol (0.4 g, 93%)). This material was used to provide **19**: ^{1}H NMR δ (DMSO-d_6) 7.49–7.52 (2H, m), 7.22–7.41 (9H, m), 6.87–6.90 (1H, m), 6.68 (1H, bs); Anal. ($C_{20}H_{16}ClNO$) C, H, N.

Bis(4-fluorophenyl)-2-fluorophenylacetamide (22). Compound **22** was prepared using 2,4′-difluorobenzophenone and 4-fluorophenylmagnesium bromide. The product was a white crystalline solid (4.98 g, 66% over 4 steps): ^{1}H NMR δ ($CDCl_3$) 7.41–7.34 (1H, m), 7.29–7.23 (4H, m), 7.16 (1H, ddd, J = 18.1, 8.1 and 1.2 Hz), 7.15 (1H, d, J = 7.7 Hz), 7.05–6.97 (4H, m), 6.93–6.87 (1H, dt, J = 8.0 and 1.4 Hz), 5.90 (1H, brs), 5.74 (1H, brs); ^{19}F NMR δ ($CDCl_3$) −103.3 (1F, s), −115.5 (2F, s); m.p 168–169 °C; Anal. ($C_{20}H_{15}F_2NO$) C, H, N.

2-(3,4-Difluorophenyl)-2,2-diphenylacetamide (23). Compound **23** was prepared using 3,4-difluorobenzophenone and phenylmagnesium bromide. The product is a white crystalline solid (160 mg, 11% over 4 steps): ^{1}H NMR δ ($CDCl_3$) 7.37–7.31 (6H, m), 7.28–7.20 (5H, m), 7.12–7.04 (2H, m), 5.90 (1H, brs), 5.74 (1H, brs); ^{19}F NMR δ ($CDCl_3$) −137.8 to −137.9 (1F, m), −140.3 to −140.4 (1F, m); mp 174–175 °C; Anal. ($C_{20}H_{15}F_2NO$) C, H, N.

2-(2,4-Difluorophenyl)-2,2-diphenylacetamide (24). Compound **24** was prepared using 2,4-difluorobenzophenone and phenylmagnesium bromide. The product is a white crystalline solid (468 mg, 32% over 4 steps): ^{1}H NMR δ ($CDCl_3$) 7.37–7.28 (10H, m), 6.95–6.83 (2H, m), 6.81–6.75 (1H, m), 5.92 (1H, brs), 5.80 (H, brs); ^{19}F NMR δ ($CDCl_3$) −99.1 (1F, dd, J = 19.2 and 8.5 Hz), −111.6 (1F, m); mp 187–188 °C; Anal. ($C_{20}H_{15}F_2NO$) C, H, N.

2,2,2-Tris-(4-fluorophenyl)-acetamide (25). Compound **25** was prepared using 4,4′-difluorobenzophenone and 4-fluorophenylmagnesium bromide. The product was crystallized from ethanol/water to afford a white crystalline solid (168 mg, 11% over 4 steps): ^{1}H NMR δ ($CDCl_3$) 7.26–7.19 (6H, dd, J = 9.0 and 5.4 Hz), 7.20–7.01 (6H, t, J =8.7 Hz), 5.83 (1H, brs), 5.69 (1H, brs); ^{19}F NMR δ ($CDCl_3$) −115.3 (F, m); mp 180–181 °C; Anal. ($C_{20}H_{14}F_3NO\cdot 0.25H_2O$) C, H, N.

2-Fluorophenyl-2,2-diphenylacetamide (30). Compound **30** was prepared using 2-fluorobenzophenone and phenylmagnesium bromide. The product is a white solid (411 mg, 27% over 4 steps): ^{1}H NMR δ ($CDCl_3$) 7.37–7.28 (6H, m), 7.15–7.05 (2H, m), 6.93 (1H, dt, J = 8.0 and 2.0 Hz), 5.90 (1H, brs), 5.68 (1H, brs); ^{19}F NMR δ ($CDCl_3$) −103.4 (F, m); mp 210 °C; Anal. ($C_{20}H_{16}FNO$) C, H, N.

4-Fluorophenyl-2,2-diphenylacetamide (31). Compound **31** was prepared using 4-fluorobenzophenone and phenylmagnesium bromide. The product is a white solid (367 mg, 24% over 4 steps): ^{1}H NMR δ ($CDCl_3$) 7.37–7.24 (12H, m), 6.97 (2H, t, J=8.5 Hz), 5.83 (1H, brs), 5.75 (1H, brs); ^{19}F NMR δ ($CDCl_3$) −116.2 (F, m); mp 193–194 °C; Anal. ($C_{20}H_{16}FNO$) C, H, N.

2,2-Bis-(3-fluorophenyl)-2-phenylacetamide (32). Compound **32** was prepared using 3,3′-difluorobenzophenone and phenylmagnesium bromide. The product is a white solid (423 mg, 23% over 4 steps): ^{1}H NMR δ ($CDCl_3$) 7.38–7.22 (7H, m), 7.09–6.96 (6H, m), 5.83 (1H, brs), 5.77 (1H, brs); ^{19}F NMR δ ($CDCl_3$) −112.6 (F, dd, J = 17.1 and 6.4 Hz); m.p 195–196 °C; Anal. ($C_{20}H_{15}F_2NO$) C, H, N.

2,2-Bis-(3-fluorophenyl)-2-(4-fluorophenyl)-acetamide (33). Compound **33** was prepared using 3,3′-difluorobenzophenone and 4-fluorophenylmagnesium bromide. The product is a brown solid (23 mg, 3% over 4 steps): ^{1}H NMR δ (DMSO-d_6) 7.60 (1H, brs), 7.34 (1H, q, J = 8.0 Hz), 7.23–7.05 (9H, m), 7.01–6.96 (2H, m), 6.87 (1H, brs); ^{19}F NMR δ ($CDCl_3$) −112.8 (1F, m), −115.7 (2F, m); Anal. ($C_{20}H_{14}F_3NO$) C, H, N.

Preparation of 3-Fluorophenyllithium. To a stirring solution of bromo-3-fluorobenzene (1.75 g, 10 mmol) in THF (25 mL) at

−78 °C was added *n*-butyllithium (4 mL, 10 mmol) dropwise. After 30 min, the solution was ready for use in the next steps.

2,2-Bis-(4-fluorophenyl)-2-(3-fluorophenyl)-acetamide (28). Compound **28** was prepared using 4,4′-difluorobenzophenone and 3-fluorophenyllithium. The product is a white solid (422 mg, 39% over 4 steps): ^{1}H NMR δ ($CDCl_3$) 7.34–7.20 (6H, m), 7.06–6.97 (6H, m), 5.90 (1H, brs), 5.71 (1H, brs); ^{19}F NMR δ ($CDCl_3$) −112.2 (1F, dd, J = 17.1 and 7.4 Hz), −115.1 to −115.2 (2F, m); mp 165–166 °C; Anal. ($C_{20}H_{14}F_3NO$) C, H, N.

2,2,2-Tris-(3-fluorophenyl)-acetamide (29). Compound **29** was prepared using 3,3′-difluorobenzophenone and 3-fluorophenyllithium. The product is a white solid (376 mg, 11% over 4 steps): ^{1}H NMR δ ($CDCl_3$) 7.35–7.21 (3H, m), 7.06–6.97 (9H, m), 7.17–7.05 (4H, m), 5.96 (1H, brs), 5.76 (1H, brs); ^{19}F NMR δ ($CDCl_3$) −112.2 (F, dd, J = 17.1 and 8.5 Hz); mp 186–188 °C; Anal. ($C_{20}H_{14}F_3NO$) C, H, N.

2,2′-Difluorobenzophenone (14). To a stirred solution of bromo-2-fluorobenzene (3.5 g, 20 mmol) in THF (50 mL) at –78 °C was added *n*-butyllithium (2.5M; 8 mL, 20 mmol) dropwise. Then after 25 min ethylformate (0.74 g, 10 mmol) was added and after 1 h the reaction was allowed to warm to 0 °C and satd NH_4Cl (aq, 30 mL) was added. To the mixture was added diethylether (60 mL), and the organic layer was washed with brine (20 mL), dried (Na_2SO_4), and concentrated under reduced pressure. The residue was purified by column chromatography (SiO_2, 100% hexane to 100% CH_2Cl_2) to afford bis-(2-fluorophenyl)methanol as a white solid (3.2 g, 73%).

A solution of bis-(2-fluorophenyl)methanol (1.09 g, 5 mmol) in dichloromethane (3 mL) was added to a slurry of PCC (3.2 g, 14 mmol) in dichloromethane (3 mL) at room temperature and stirred vigorously overnight. The slurry was filtered through a short silica\celite plug to remove excess PCC. The eluent was concentrated and purified by column chromatography (SiO_2, hexanes/dichloromethane; 3:1). The product **14** was a white solid (0.93 g, 87%). Analysis agreed with reported data.[25]

2,2-Bis-(2-fluorophenyl)-2-phenylacetamide (26). Compound **26** was prepared using 2,2′-difluorobenzophenone and phenylmagnesium bromide. The product is a white solid (236 mg, 17% over 4 steps): ^{1}H NMR δ ($CDCl_3$) 7.39–7.27 (9H, m), 7.17–7.03 (4H, m), 5.90 (1H, brs), 5.85 (1H, brs); ^{19}F NMR δ ($CDCl_3$) −102.9 (F, m); mp 166–167 °C; Anal. ($C_{20}H_{15}F_2NO$) C, H, N.

2,2-Bis-(2-fluorophenyl)-2-(4-fluorophenyl)-acetamide (27). Compound **27** was prepared using 2,2′-difluorobenzophenone and 4-fluorophenylmagnesium bromide. The product is a white solid (147 mg, 14% over 4 steps): ^{1}H NMR δ ($CDCl_3$) 7.41–7.34 (2H, m), 7.29–7.23 (4H, m), 7.17–7.05 (4H, m), 6.99 (2H, t, J = 8.7 Hz), 5.78 (2H, brs); ^{19}F NMR δ ($CDCl_3$) −103.0 (2F, m), −115.9 (1F, m); mp l87–188 °C; Anal. ($C_{20}H_{14}F_3NO$) C, H, N.

Washed Red Blood Cell Assay (Gardos Channel Inhibition). Heparinized human blood was obtained from Biological Specialty Corp. The whole blood was initially diluted 1:1 with Modified Flux Buffer (MFB). MFB consists of 140 mM NaCl, 5 mM KCl, 10 mM Tris, 0.1 mM EGTA (pH = 7.4). The blood was centrifuged at 1000 rpm and the pellet consisting of predominantly red blood cells (RBCs) was washed three times with MFB. The cells were then loaded with ^{86}Rb by incubating the washed cells with ^{86}Rb at a final concentration of 5 μCi/mL for at least 3 h at 37 °C. After loading with ^{86}Rb, the RBCs were washed three times with chilled MFB. The cells were then incubated for 10 min with test compound at concentrations that ranged between 1 and 10000 nM. Efflux of ^{86}Rb was initiated by raising intracellular calcium levels in the RBCs by addition of $CaCl_2$ and A23187 to final concentrations of 2 mM and 5 μM, respectively. After 10 min, the RBCs were pelleted in a microfuge and the supernatant was removed and counted in a Wallac MicroBeta liquid scintillation counter. Percent inhibition of efflux and IC_{50} values through the Gardos channel were then calculated. The above protocol is a modification of the protocol for measurement of Gardos channel inhibition in RBCs reported previously.[11] IC_{50} values were calculated using the Origin software logistic function (Microcal Software, Northampton, MA).

Solubility and Rat S9-Metabolism Studies. Intrinsic microsomal clearance (Cl_{int}) was determined using the S9 fraction of liver Biosciences). Compounds were incubated at 37 °C in a shaking water bath for 15 and 30 min. The concentration of each compound was determined by LC/MS/MS after reaction quenching with acetonitrile (Table 2).

The solubility of compounds was determined with a modified shake-flask method. Typically, 1 mg of compound was shaken overnight in 1 mL of phosphate-buffered saline (pH 6.8). The supernatant was removed and analyzed for compound by LC/MS/MS.

In Vivo Pharmacokinetic Studies. To determine the plasma kinetics of compounds **10**, **19**, and **21**, the compounds were administered either by intravenous (IV) injection (tail vein) or by oral gavage (PO) to a set of 18 groups (n = 3 per time point) of male Sprague–Dawley rats weighing 251–299 g. The compounds were administered on Day 1 at a dose level of 1 mg/Kg (IV) or 10 mg/Kg (PO), with dose volumes of 1 mL/Kg (IV), and 2 mL/Kg (PO), respectively. A solution of each compound in a PEG-400/cremophor-EL (both from Sigma Chemical Company, St. Louis, Missouri) vehicle was used for the IV arm, while a 0.5% aqueous solution of methylcellulose (from Sigma Chemical Company, St. Louis, Missouri) was used for the oral arm of the study. Blood samples were obtained at 0.08, 0.25, 0.5, 1, 2, 4, 6, 8, 12, and 24 h post IV administration and at 0.5, 1, 2, 4, 6, 8, 12, and 24 h post PO administration. Quantification of compound concentrations in plasma was accomplished by LC-MS (Figure 2).

Studies in Transgenic Sickle (SAD-1) Mice. Transgenic SAD-1 females and males between 3 and 6 months of age, weighing 25−30 g, were used for this study. The SAD-1 mice were divided into two groups, and either vehicle or compound (**10**, 20 mg/kg, bid, or **21**, 10/mg/kg, bid) was administered by oral gavage. Hematological parameters were evaluated at baseline and days 7 and 14 for compound **10**, and baseline and days 11 and 21 for compound **21**. Blood sampling and vehicle administration have previously been shown not to affect the blood parameters measured in this study (Table 3).[13]

Hematological Data from SAD-1 Mice. Blood samples were obtained at specific intervals and were used for $^{86}Rb^+$ influx measurements, determination of red blood cell (RBC) phthalate density distribution curves, cell morphology studies, determination of RBC cation content, and other hematological parameters. The hemoglobin (Hb) concentration was determined by the spectroscopic measurement of the cyanmet derivative. The hematocrit (Hct) was determined by centrifugation in a micro-Hct centrifuge. The cells were washed three times with PBS (330 mOsm) at 25 °C in 2 mL tubes. Density distribution curves and median RBC densities (D_{50}) were obtained according to Danon and Marikovsky using phthalate esters in microhematocrit tubes.[26]

Acknowledgment. We would like to thank Dr. Carlo Brugnara for insightful discussion regarding SCD and the SAD-1 mouse model.

Supporting Information Available: Supplemental analytical and pharmacokinetic data and experimental procedures. This material is available free of charge via the Internet at http://pubs.acs.org.

References

(1) Brittenham, G. M.; Schechter, A. N.; Noguchi, C. T. Hemoglobin S polymerization: Primary determinant of hemolytic and clinical severity of the sickling syndromes. *Blood* **1985**, *65*, 183–189.

(2) Fabry, M. E.; Costantini, F.; Pachnis, A.; Suzuka, S. M.; Bank, N.; Aynedjian, H. P.; Factor, S. M.; Nagel, R. L. High expression of human β^S- and α-globins in transgenic mice: Erythrocyte abnormalities, organ damage, and the effect of hypoxia. *Proc. Natl. Acad. Sci. U.S.A.* **1992**, *89*, 12155–12159.

(3) Eaton, W. A.; Hofrichter, J. Hemoglobin S gelation and cell sickle cell disease. *Blood* **1987**, *70*, 1245–1266.

(4) Serjeant, G. R.; Serjeant, B. E.; Milner, P. F. The irreversibly sickled cell: A determinant of hemolysis in sickle cell anemia. *Br. J. Hamaetol.* **1969**, *17*, 527–533.

(5) Glader, B. E.; Nathan, D. G. Cation permeability alterations during sickling: relationship to cation composition and cellular hydration of irreversibly sickled cells. *Blood* **1978**, *51*, 983–989.
(6) Gardos, G. The function of calcium in the potassium permeability of human erythrocytes. *Biochim. Biophys. Acta* **1958**, *30*, 653–654.
(7) Ishii, T. M.; Siliva, C.; Hirschberg, B.; Bond, C. T.; Adelman, J. P.; Maylie, J. A human intermediate conductance calcium-activated potassium channel. *Proc. Natl. Acad. Sci. U.S.A.* **1997**, *94*, 11651–11656.
(8) Grygorczyk, R.; Schwarz, W.; Passow, H. Ca^{2+}-Activated K^+ channels in human red blood cell. *Biophys. J.* **1984**, *45*, 693–698.
(9) McGoron, A. J.; Joiner, C. H.; Palascak, M. B.; Claussen, W. J.; Franco, R. S. Dehydration of mature and immature sickle red blood cells during fast oxygenation/deoxygenation cycles: role of K-Cl cotransport and extracellular calcium. *Blood* **2000**, *95*, 2164–2168.
(10) Dunn, P. M. The action of blocking agents applied to the inner face of Ca^{2+}-activated K^+ channels from human erythrocytes. *J. Membr. Biol.* **1998**, *165*, 133–43.
(11) Brugnara, C.; de Franceschi, L.; Alper, S. L. Inhibition of Ca^{2+}-dependent K^+ transport in sickle cell erythrocytes by clotrimazole and other imidazole derivatives. *J. Clin. Invest.* **1993**, *92*, 520–526.
(12) Coupry, I.; Armsby, C. C.; Alper, S. L.; Brugnara, C.; Parini, A. Clotrimazole and Efaroxan inhibit red cell Gardos channel independently of imidazoline I_1 and I_2 binding sites. *Eur. J. Pharmacol.* **1996**, *295*, 109–112.
(13) de Franceschi, L.; Beuzard, Y.; Brugnara, C. Sulfydryl oxidation and activation of red cell K^+Cl^- cotransport in the transgenic SAD mouse. *Am. J. Physiol.* **1995**, *269*, C899–906.
(14) de Franceschi, L.; Saadane, N.; Trudel, M.; Alper, S. L. Inhibition of Ca^{2+} activated K^+ transport and reverses erythrocyte dehydration in transgenic SAD mice. A model for therapy of sickle cell disease. *J. Clin. Invest.* **1994**, *93*, 1670–1676.
(15) Fowler, S. M.; Riley, R. J.; Pritchard, M. P.; Sutcliffe, M. J.; Friedberg, T.; Wolf, R. C. Amino acid 305 determines catalytic center accessibility in CYP3A4. *Biochemistry* **2000**, *39*, 4406–4414.
(16) Brugnara, C.; Armsby, C. C.; Sakamoto, M.; Rifai, N.; Alper, S.; Platt, O. Oral administration of clotrimazole and blockade of human erythroctes Ca^{+2}-activated K^+ channel: The imidazole ring is not required for inhibitory activity. *J. Pharm. Exp. Ther.* **1995**, *273*, 266–272.
(17) Alvarez, J.; Montero, M.; Garica-Sancho, J. High affinity inhibition of Ca^{2+}-dependent K^+ channels by cytochrome P-450 inhibitors. *J. Biol. Chem.* **1992**, *267*, 11789–11793.
(18) Ashcroft, F. M. *Ion Channels and Disease*; Academic Press: New York, 2000; pp 117–123.
(19) Burgess, E. M.; Penton, H. R.; Taylor, E. A. Thermal reactions of alkyl *N*-carbomethoxysulfamate esters. *J. Org. Chem.* **1973**, *38*, 26–31.
(20) Klumpp, D. A.; Yeung, K. Y.; Prakash, G. K. S.; Olah, G. Preparation of 3,3-diaryloxindoles by superacid-induced condensations of isatins and aromatics with a combinatorial approach. *J. Org. Chem.* **1998**, *63*, 4481–4484.
(21) Herold, F.; Wolska, I.; Helbin, E.; Krol, M.; Kleps., J. Synthesis and structure of novel 4-arylhexahydro-1*H*,3*H*-pyrido[1,2-*c*]pyrimidine derivatives. *J. Heterocycl. Chem.* **1999**, *36*, 389–396.
(22) Franco, M. L. T. M. B.; Herold, B. J.; Evans, J. C.; Rowlands, C. C. Substituent effects on electron spin distribution and conformation of radical ions obtained from 9-diphenylmethylenefluorenes. *J. Chem. Soc., Perkins Trans. 2* **1988**, *443*–449.
(23) Stocker, J.; de Franceshi, L.; McNaughton-Smith, G. A.; Brugnara, C. A novel Gardos channel inhibitor, ICA-17043, prevents red blood cell dehydration in vitro and in a mouse model (SAD) of sickle cell disease. *Blood* **2000**, *96*, 486A.
(24) Stocker, J.; De Franceschi, L.; McNaughton-Smith, G.; Corrocher, R.; Beuzard, Y.; Brugnara, C. ICA-17043, a novel Gardos channel blocker, prevents sickled red blood cell dehydration in vitro and in vivo in SAD mice. *Blood* **2003**, *101*, 2412–2418.
(25) Riechers, H.; Albrecht, H.-P.; Amberg, W.; Baumann, E; Bernard, H.; Böhm, H.-J.; Klinge, D.; Kling, A.; Muller, S.; Raschack, M.; Unger, L.; Walker, N.; Wernet, W. *J. Med. Chem.* **1996**, *39*, 2123–2128.
(26) Danon, D.; Marikovsky, Y. Determination of density distribution of red blood population. *J. Lab. Clin. Med.* **1964**, *64*, 668–674.

JM070663S